Pool Fire Plume Flow in a Large-Scale Wind Tunnel

V. B. APTE and A. R. GREEN
Londonderry Occupational Safety Centre
132 Londonderry Road, Londonderry, N.S.W. 2753, Australia

J. H. KENT
Mechanical Engineering Department
University of Sydney, N.S.W. 2006, Australia

ABSTRACT

Transient characteristics of plume flows generated by 0.57 m-2.0 m diameter aviation fuel pool fires in a 5.4 m wide x 2.4 m high x 130 m long tunnel for ventilation rates in the range of 0.5-2.0 m/s have been measured and predicted using a mathematical model. The objective was to simulate and understand the transport of combustion products of a fire in a ventilated mine roadway network with a view to determine the optimum wind rate, fire alarm sitings, escape routes, etc. A stratified layer of hot combustion products was formed near the ceiling and flowed against the ventilation at sufficiently low wind speeds. The backflow was arrested as the wind speed was increased, and the critical wind speed required to stop the backflow was higher for larger fires. The measured fuel pyrolysis mass loss flux ($\dot{m}''$) was observed to increase with the pool diameter. At higher wind speeds, $\dot{m}''$ decreased as the flame tilted away from the pool surface, reducing the heat feedback.

Predictions of the temperature and flow fields (including the backflow) and flame geometry made by a 3-dimensional k-ϵ turbulence combustion model [1] in the steady state regime of the fire agree generally well with the measurements.

KEYWORDS : Fire plume ; Pool fire ; Wind tunnel

NOTATION

a_g	Gravitational acceleration
f	Mixture fraction
g	Mixture fraction fluctuation variance
h	Enthalpy

k	Turbulence kinetic energy
$\dot{m}''$	Fuel mass pyrolysis flux
P	Pressure
S_ϕ	Source/sink term
$u,v,w,$	Velocity components along x,y and z directions
x,y,z	Distance along tunnel length, width and height respectively
Γ_ϕ	Exchange coefficient for ϕ
ϵ	Turbulence dissipation rate
μ_t	Effective viscosity
ρ	Density
σ_ϕ	Turbulent Prandtl/Schmidt number
ϕ	Any variable

INTRODUCTION

Dissemination of hot and toxic combustion products of a fire in a mine roadway network poses a major threat to the lives of miners. Besides taking measures to prevent and control such fires, it is imperative to design an efficient fire detection system and safe escape routes. To achieve this, it is necessary to be able to accurately predict the movement and distribution of fire products in a ventilation network. Current fire programmes for mine networks [2] make unrealistic assumptions on fire behaviour and ignore the multidimensionality of real fires. Prediction methods will be helpful in assessing practical measures to prevent a backflow of combustion products and ensure that they move in the required direction and not end up in the areas used for egress.

In line with this ideology, pool fire tests have been conducted in a full-scale fire gallery at the Londonderry Occupational Safety Centre, N.S.W., Australia for varying ventilation rates and fire sizes. The time varying aspects of the fire plume flow (e.g., the temperature and flow fields, flame geometry, burning rate, etc.) were measured. Using the burning rate as an input to a 3-dimensional k-ϵ turbulence model incorporating combustion, the temperature and flow fields and the flame profile were predicted and compared with measurements.

Earlier work on thermally generated stratified smoke layers in wind tunnels includes 2-dimensional models and their validations using small-medium scale experiments [3- 6]. The present study models the movement of combustion products generated by ventilated fires in a full-scale tunnel. This paper presents only a part of our ongoing work and a more extensive analysis of the results will be presented at a later date.

EXPERIMENTAL

The experiments were conducted in a 130 m long tunnel with a cross-section 5.4 m wide x 2.4 m high, simulating a typical Australian mine roadway on a 1:1 scale. Air flow was created in the tunnel by two exhaust fans installed at one end of the tunnel, maintaining a sub-atmospheric tunnel pressure. The flow entering the tunnel through

the opposite end was measured by a set of orifice plates attached to the door. A wooden gate with a 70% open rectangular grid was located 12 m from the door for flow straightening. Further along the flow at 40 m was the fuel pool, and 70 m downwind of the pool was an oxygen depletion calorimeter with orifice plates to measure the total plume flow. Details of the tunnel and its flow measuring systems are given elsewhere [7].

A three dimensional array of 84 thermocouples (chromel-alumel, type K, 1200°C range) was arranged around the pool, to a distance of 13 m upstream and 40 m downstream of the fire. An array of 24 bidirectional probes arranged in the vertical plane coincident with the centreline of the flow front and covering a distance of 13 m on both sides of the fire measured both forward and reverse point velocities. Two video cameras, one viewing the fire along the flow and the other looking from a side perpendicular to the flow measured the size and the angle of the flame. The mass loss of the burning fuel was measured by load cells placed under the three legs of a platform supporting the fuel tray. The load cells were shielded and aircooled to prevent overheating.

The experiments were conducted using aviation fuel floating over a 20 mm water layer in 0.57 - 2 m diameter trays, under ventilation rates of up to 2 m/s as measured prior to the burn upstream of the fire. Data on the temperature and the flow fields, fuel burning rate, and the total air flow upstream and downstream of the fire were logged on a computer.

THEORETICAL TREATMENT

The flow is described by the three dimensional time mean equations of transport for mass, momentum, gas species and enthalpy. Turbulent viscosity and diffusivities are handled by the k-ϵ model [8] which requires two additional transport equations in turbulent energy and dissipation. All equations are coupled by the gas density, which is a function of enthalpy and the gas molecular weight from the combustion model.

The equations are cast in the following common form [9] :

$$\text{div} (\varrho \hat{u} \phi) = \text{div} (\Gamma_\phi \text{ grad } \phi) + S_\phi \qquad (1)$$

Here, ϕ represents the three velocity components u, v, w, the turbulence quantities k and ϵ, enthalpy h, the conserved scaler mixture fraction f [10, 11] and the variance of mixture fraction fluctuations g [12]. Also $\phi = 1$ represents global continuity. In all there are nine conservation equations to be solved.

The effective turbulent viscosity is $\mu_t = C_\mu \varrho k^2 / \epsilon$.

The term S_ϕ represents source or sink terms in these equations and also flux terms in the momentum equations which do not fit conveniently into the form of Eq. 1. The terms are shown in Table 1. Buoyancy forces appear in the vertical momentum equation.

Combustion is modelled in the gas phase using the mixture fraction concept. The fuel is liquid and evaporates at the surface to give a gas

phase fuel which burns as a turbulent diffusion flame in air. The fundamental assumption of the method is that the combustion reaction rate is determined by the gas mixing rate of fuel with air. The chemical kinetics rates are much faster than the gas mixing rates and a thin instantaneous reaction zone is formed. Then, assuming that the turbulent diffusivities of all gas species are equal, the mass fraction

TABLE 1. Flux and Source Terms for Transport Equations.

Φ	Γ_Φ	S_Φ
1	o	o
u	μ_t	$-\frac{\partial P}{\partial x} + \frac{\partial}{\partial x}\left(\mu_t \frac{\partial u}{\partial x}\right) + \frac{\partial}{\partial y}\left(\mu_t \frac{\partial v}{\partial x}\right) + \frac{\partial}{\partial z}\left(\mu_t \frac{\partial w}{\partial x}\right)$
v	μ_t	$-\frac{\partial P}{\partial y} + \frac{\partial}{\partial x}\left(\mu_t \frac{\partial u}{\partial y}\right) + \frac{\partial}{\partial y}\left(\mu_t \frac{\partial v}{\partial y}\right) + \frac{\partial}{\partial z}\left(\mu_t \frac{\partial w}{\partial y}\right)$
w	μ_t	$-\frac{\partial P}{\partial z} + \frac{\partial}{\partial x}\left(\mu_t \frac{\partial u}{\partial z}\right) + \frac{\partial}{\partial y}\left(\mu_t \frac{\partial v}{\partial z}\right) + \frac{\partial}{\partial z}\left(\mu_t \frac{\partial w}{\partial z}\right) + a_g(\rho_{ref} - \rho)$
k	μ_t/σ_k	$G_k - \rho\epsilon$
ϵ	μ_t/σ_ϵ	$(C_1 G_k - C_2 \rho \epsilon)\, \epsilon/k$
f	μ_t/σ_f	0
g	μ_t/σ_g	$C_{g1}\left[\left(\frac{\partial f}{\partial x}\right)^2 + \left(\frac{\partial f}{\partial y}\right)^2 + \left(\frac{\partial f}{\partial z}\right)^2\right] - C_{g2}\, \rho\, g\epsilon/k$
h	μ_t/σ_h	0

$$G_k = \mu\left[2\left\{\left(\frac{\partial u}{\partial x}\right)^2 + \left(\frac{\partial v}{\partial y}\right)^2 + \left(\frac{\partial w}{\partial z}\right)^2\right\} + \left(\frac{\partial u}{\partial y} + \frac{\partial v}{\partial x}\right)^2 + \left(\frac{\partial v}{\partial z} + \frac{\partial w}{\partial y}\right)^2 + \left(\frac{\partial u}{\partial z} + \frac{\partial w}{\partial x}\right)^2\right]$$

C_μ	C_1	C_2	C_{g1}	C_{g2}
0.09	1.44	1.92	2.8	2.0

σ_k	σ_ϵ	σ_f	σ_g	σ_h
0.9	1.22	0.7	0.7	0.7

of any species can be expressed in terms of a chemically conserved variable termed the mixture fraction. Here we choose the mass fraction of the fuel elements to be the mixture fraction. It has a value of unity in the pure fuel, zero in air and at the reaction zone it is the stoichiometric mass fraction of fuel in the air-fuel mixture [10, 11].

Combustion is modelled as a one step reaction to completion forming carbon dioxide and water as the products. Details of minor gaseous products are not required for the present analysis and these products have little effect on the temperature and density fields. Thus in the present model no fuel is found on the air side of the stoichiometric value of mixture fraction and no oxygen is found on the fuel side. Algebraic relations can be obtained between mixture fraction and gas species using the above assumptions and the solution of the mixture fraction equation leads to specification of the species concentrations and gas molecular weight.

The fuel used here is modelled as octane. The enthalpy of reaction used is only 30 MJ/kg which takes account of radiation losses and incomplete combustion due to soot formation [13]. The justification for omitting detailed radiation modelling is that most of the flux is absorbed at the walls of the tunnel which become hot. Little of this energy comes back into the flow upstream of the fire by wall convection. Thus the radiant energy is largely lost by our system. This is modelled as a reduced enthalpy of reaction with adiabatic conditions at the walls.

Turbulent fluctuations of the mixture fraction and the instantaneous reaction zone location are modelled using the g equation, the variance of fluctuations in mixture fraction [12]. A limited Gaussian probability distribution function is assumed for the scalar fluctuations. The average specific volume at a point in space is obtained by integrating the instantaneous function of mixture fraction over the Gaussian probability distribution function [10].

The equations are solved numerically using a finite volume first order differencing scheme [9]. Hybrid upwind differencing is used when the cell Peclet number exceeds 2. The equations are linearized where possible in terms of the current variable to be solved, so as to use an implicit differencing scheme. Additional terms are put into the source term and use the previous iteration values. Iterations are performed using a tridiagonal matrix solver and suitable underrelaxation factors. The numerical grid is 89 x 10 x 12 and is refined in the pool region.

The upstream boundary is 40 m from the pool and the exit boundary is 50 m downstream of the pool. At the upstream end, zero gradients for all variables in the flow direction are specified. The mass flow rate at the inlet grid cells is allowed to float with the provision that the overall mass flow rate balances the fan outflow. This allows reverse flow (outflow) to take place at this boundary under conditions of low suction draft from the fans at the outlet. Leakages of air into the gallery from the side walls are modelled by additional air ports in the appropriate locations. Standard turbulent boundary layer velocity profiles are modelled at the walls.

The air mass flow rates and the fuel burning rate are specified from the measured values. The conditions are : upstream air in 13.9 kg/s, leakage air in at side walls 4.0 kg/s and fuel burning rate 0.066 kg/s.

Satisfactory convergence of the numerical scheme was achieved after about 300 iterations. This took about two hours elapsed time using a Stardent Titan computer.

RESULTS AND DISCUSSIONS

Five tests have been selected as indicated in Table 2 to demonstrate the effects of wind velocity (Tests 1, 2 and 3) and pool diameter (Tests 4, 2 and 5). Predictions using the mathematical model will be presented for Test 2 at 800 seconds from ignition, i.e., during the steady state regime as will be seen in the following sections.

TABLE 2. Data on Experimental Conditions

Test No. Same as Curve No. on Fig 1	Pool Diameter (m)	Upstream Wind Velocity (m/s)	Angle of Flame tilt to vertical during steady state (Deg.)	
			Measured	Predicted
1	1.0	0.5	54	20
2	1.0	0.85	59	30
3	1.0	2.0	66	36
4	0.57	0.9		
5	2.0	0.85		

Burning Rate

Figure 1 shows the effects of the wind velocity and the pool diameter on the measured fuel mass loss flux ($\dot{m}''$).

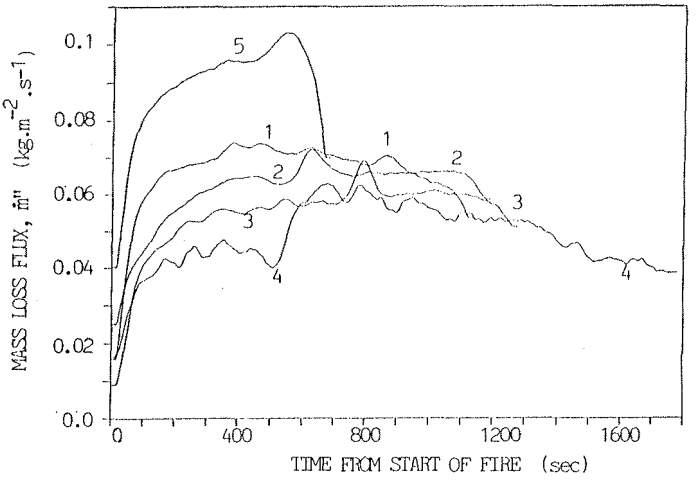

FIGURE 1. Effect of wind flow and pool size on transient burning rate (See TABLE 2 for conditions of Tests 1- 5).

The $\dot{m}''$ is calculated by dividing the burning rate (obtained as the slope of the fuel mass vs. time curve) by the pool area. The burning rate rapidly increases to a relatively steady value and decays as the fuel runs out. For the 1 m pool diameter tests (curves 1-3), a four-fold increase in the wind velocity (from 0.5 to 2 m/s) causes the steady state $\dot{m}''$ value (at 450 sec.) to fall by nearly 25% (from 0.072 to 0.054 kg $m^{-2}s^{-1}$). This may be explained by the observed increase in the angle of flame tilt to the vertical (see Table 2) with the wind speed, which would reduce the flame-fuel surface heat flux, therefore decreasing $\dot{m}''$. For the pool diameter increasing by a factor of 3.5, $\dot{m}''$ in the steady state regime is seen to rise by over a factor of 2 (compare curves 4, 2 and 5 at 400 sec.).

Temperature Field

Propagation of hot combustion gases along the tunnel is shown on Figs. 2a-f as temperature fields measured at increasing times during the fire over the vertical X-Z plane cutting through the centre of the fire.

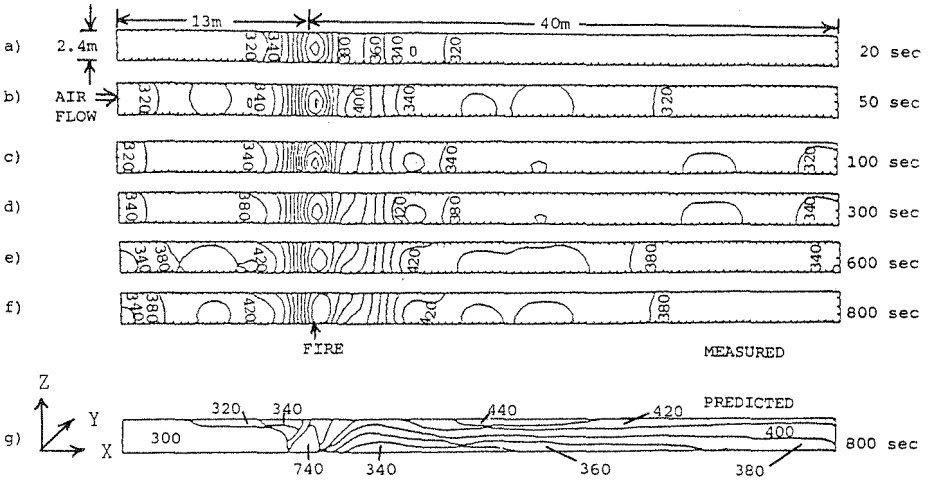

FIGURE 2. Measured (a-f) and predicted (g) temperature fields for Test 2 (temperature in K, time in seconds from ignition).

Within 300 seconds from ignition, the 340 K temperature front is seen to move 40 m downwind and 2 m upwind of the fire. Beyond 600 seconds, the temperatures become relatively steady along with the burning rate (curve 2, Fig. 1).

The predicted temperature field (Fig. 2g) downwind of the fire is more stratified as compared to the measurements (Fig. 2f), though the overall temperature in this region is reasonably well predicted. Temperatures upstream of the fire are much underpredicted.

Flow Field

Figure 3a shows the velocity field over the same plane as Fig. 2, estimated from the measured pressure drop across the bidirectional probes and the temperature (to give the local density).

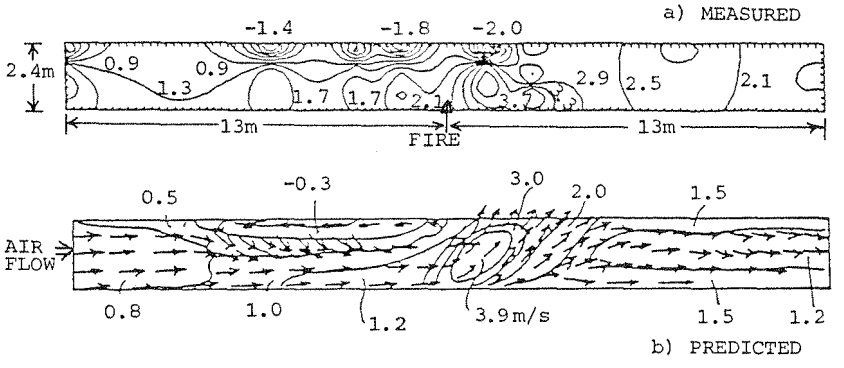

FIGURE 3. Measured (a) and predicted (b) velocity fields for Test 2 (Velocity in m/s, time : 800 seconds from ignition).

The total mass flow computed by integrating these measurements is about 30 % higher than that measured with the orifice plates in the oxygen depletion calorimeter downwind of the fire. A substantial backflow along the ceiling is observed on Fig. 3a. The predicted velocities on Fig. 3b compare fairly with the measurements in the downwind and the lower upwind regions. The backflow is underpredicted similar to the corresponding temperature field before the fire (Fig. 2g).

As the upstream wind flow was increased to 2 m/s (Test 3, Table 2), the smoke backflow was arrested. For the large fire of test 5, the extent of measured backflow was much greater than that of test 2.

Mixture Fraction and Oxygen Concentration

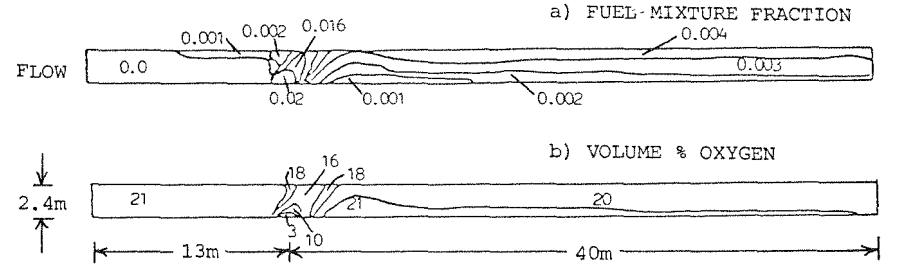

FIGURE 4. Predicted fuel mixture fraction (a) and oxygen concentration (b) fields for Test 2 (Correspond to Fig. 2g).

Model predictions of the fuel mixture fraction and the percent volumetric oxygen concentration fields are presented on Figs. 4a and 4b respectively. These correspond to Fig. 2g.

As we go away from the fire, the fuel concentration rapidly drops (Fig. 4a) becoming negligible in the bulk flow and the oxygen level rises sharply, approaching the ambient volumetric concentration of 21% (Fig. 4b).

CONCLUDING REMARKS

The present approach enables us to predict the spread of combustion products of a fire in a tunnel for known ventilation rates and fire sizes. The model is validated against full-scale data, eliminating scaling problems. The results can be used to assess the hazards posed by the heat and toxicity of gases produced by fires in mine roadways and similar long enclosures of public thoroughfare. Accordingly, fire alarms and evacuation outlets can be appropriately located and ventilation rates to prevent smoke backflow into escape areas can be recommended. There is a scope to improve the predictions of the present model with parametric studies. Further experiments are needed using criss-crossing tunnels to simulate a mine network. Work along these lines is in progress.

ACKNOWLEDGEMENTS

The authors wish to thank the National Energy Research, Development and Demonstration Council of Australia, and the Workcover Authority of New South Wales for the funding provided for this work. Thanks are also due to Mr. Yuva Raja Upadhyaya and Mr. Les Golder for their technical assistance during the experiments.

REFERENCES

1. Boyd, R.K. and Kent, J.H.,"Three-Dimensional Furnace Computer Modelling", 21st Symposium (International) on Combustion, The combustion Institute, Pittsburgh: 265- 274, 1986.

2. Chang, X., Laage, L.W. and Greuer, R.E. "A User's Manual for MFIRE: A Computer Simulation Program for Mine Ventilation and Fire Modeling", Information Circular 9245, US Deptartment of Interior, Bureau of Mines, 1990.

3. Ku, A.C., Doria, M.L. and Lloyd, J.R., "Numerical Modeling of Unsteady Buoyant Flows Generated by Fire in a Corridor", 16th Symposium (International) on Comb., The Combustion Institute, Pittsburgh : 1373- 1384, 1976.

4. Hwang, C.C., Chaiken, R.F., Singer, J.M. and Chi, D.N.H. "Reverse Stratified Flow in Duct Fires : A Two-Dimensional Approach", 16th Symposium (International) on Comb., The Combustion Institute, Pittsburgh : 1385- 1395, 1976.

5. Bos, W.G., Van Den Elsen, T., Hoogendoorn, C.J. and Test,F.L. "Numerical Study of Stratification of Smoke Layer in a Corridor", Comb. Sci. Tech., 38 : 227- 243, 1984.

6. Hwang, C.C. and Wargo, J.D., "Experimental Study of Thermally Generated Reverse Stratified Layers in a Fire Tunnel", Comb. Flame, 66 : 171- 180, 1986.

7. Apte, V.B. and Bilger, R.W., "Measurement and Control of Air Flow in the Fire Gallery at Londonderry Occupational Safety Centre", Contract Report F-15, Mechanical Engineering Department, Sydney University, Australia, 1987.

8. Launder, B.E., Morse, A., Rodi, W. and Spalding, D.B., "The Prediction of Free Shear Flows- a Comparison of Six Turbulence Models", NASA Free Shear Conference, NASA Report No. SP-311, 1972.

9. Patankar, S.V., Numerical heat transfer and fluid flow, Hemisphere, 1980.

10. Bilger, R.W., "Turbulent Jet Diffusion Flames", Prog. in Energy Comb. Sci. 1: 87, 1976.

11. Kent, J.H. and Bilger, R.W., "The Prediction of Turbulent Diffusion Flames and Nitric Oxide Formation" 16th Symposium (International) on Comb., The Combustion Institute, Pittsburgh : 1643- 1656, 1976.

12. Spalding, D.B., "Concentration Fluctuations in a Round Turbulent Free Jet", Chem. Eng. Sci. 26 : 95, 1971.

13. Kent, J.H. and Honnery, D., "Soot and Mixture Fraction in Turbulent Diffusioin Flames", Comb. Sci. Tech. 54 : 383- 397, 1987.